Identification of time-varying signals in quantum systems

Xi Cao,[1] Yu-xi Liu,[2] and Re-Bing Wu[1,*]
[1]*Department of Automation, Tsinghua University, Beijing 100084, China*
[2]*Institute of Microelectronics, Tsinghua University, Beijing 100084, China*

(Received 19 February 2020; revised 24 December 2020; accepted 25 January 2021; published 22 February 2021)

The identification of time-varying parameters (e.g., directly inaccessible *in situ* signals in vacuum and low-temperature environments) is prevalent for characterizing the dynamics of quantum processes. Under certain circumstances, they can be identified from time-resolved measurements via Ramsey interferometry experiments, but only with specially designed probe systems can the parameters be explicitly read out, and a rigorous identifiability analysis is lacking, i.e., whether the measurement data are sufficient for unambiguous identification. In this paper we formulate this problem as the invertibility of the input-output mapping associated with the quantum system for which an algebraic identifiability criterion is derived based on the system's relative degree. The invertibility analysis also leads to an inversion-based algorithm for numerically identifying the parameters, which is computationally much more efficient than nonlinear regression methods. The effectiveness of the criterion are demonstrated by numerical examples.

DOI: 10.1103/PhysRevA.103.022612

I. INTRODUCTION

The full characterization of quantum dynamics is crucial for high-precision modeling and manipulation of quantum information processing systems. In the literature, extensive studies have been cast to the identification of quantum states and operations (known as quantum state and process tomography) [1–3] or quantum Hamiltonians [4–10]. Most of these works focus on the estimation of constant but unknown quantities, e.g., a density or process matrix [4–8,11,12] or some parameters in the Hamiltonian [9–11,13], based on maximum likelihood [11,14], regression [12,13], or compressive sensing estimators [4–10]. However, the identification of unknown time-varying parameters has been rarely studied. Such problems broadly exist in low-temperature quantum information processing systems in which many signals are not directly accessible by ambient measurement devices. For the example of superconducting quantum chips [15] shown in Fig. 1, the *in situ* dc or ac control signals in low-temperature environments always experience distortion by attenuators and control lines or crosstalks between them [15–25], but the distorted signals are directly accessible by a room-temperature measurement apparatus.

To calibrate the distortion, it is necessary to identify the real distorted signals in quantum systems that are not directly accessible by measurement devices. Such signals must be indirectly extracted from available measurements on the quantum system that they interact with. For instance, some *in situ* signals can be readout from the qubit phase variance measured by Ramsey experiments (see Sec. II) [26–29], but such a scheme is not generalizable to more complicated systems. More seriously, as will be shown in Sec. II, such a method is problematic as it leads to nonunique estimations. Alternatively, nonlinear regression method [13] can be applied to identify time-varying signals by curve fitting via the dynamical model, but there are various numerical issues such as high computational cost and failed estimation due to improperly selected initial guesses. Moreover, whether the signal can be uniquely determined by a given measurement scheme, which is termed as the identifiability of the signals, is still not well understood in these methods.

Therefore a method that is computationally economic, stable, and with guaranteed identifiability is demanded in practice. From a system point of view, the identification of time-varying parameters from time-varying measurements can be thought of as reversing the system's input-output mapping [30]. Whether the parameters are identifiable is equivalent to the left invertibility of the system (Chap. 5, [31]), i.e., the property that different inputs must produce different outputs. In parallel, the right invertibility (Chap. 5, [31]) is referred to as the property that any desired time-varying output can be produced by some (nonunique) input function. In the classical domain, the left invertibility was applied for estimating the source of heat conduction from temperature measurements [32], while the right invertibility was often used for designing tracking control of a robot along a chosen trajectory [33]. All studies collectively showed that the invertibility of a general input-output system is determined by its relative degree that can be specified by an inversion algorithm.

In the quantum domain, the left invertibility was first studied by Ong *et al.* [34] in a nonlinear filtering problem based on nondemolition continuous-time measurements. This work showed that under adequate Lie algebraic conditions the time-varying input of a quantum system can be recovered in real time from the time trace of a continuously measured

*rbwu@tsinghua.edu.cn

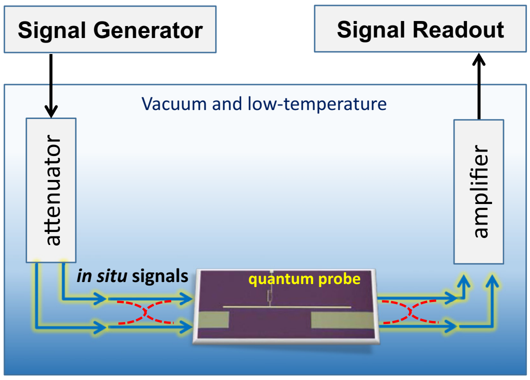

FIG. 1. Schematic diagram of the identification of time-varying signals in a superconducting quantum computing system. The *in situ* signals are delivered from ambient signal generators that experience distortion and crosstalk, but the actual signals are not accessible by room-temperature devices. A quantum probe (e.g., a superconducting qubit) is placed to receive the signal, whose measurement signals are conducted out for identifying the *in situ* signals.

observable. Later on, the inversion (of right invertible systems) was applied to the quantum control design as a reference tracking problem based on virtual feedback [35–40] or to the estimation of quantum states and Hamiltonians [7,9].

In this paper we will apply the inversion-based method to the identification of time-varying parameters. This can be treated as a generalization of the work of Refs. [34,41], but the measurements do not have to be nondemolitional because the time-resolved output signal can be measured via ensemble average. We will also extend the invertibility criterion and inversion algorithm from the single signal case to more complicated multisignal cases, which are much more complicated and have not been explored in the literature. These cases are prevalent in multiqubit systems that are coupled with multiple signals.

The remainder of this paper will be organized as follows. Section II shows how the ambiguity issue arises in direct Ramsey-based identification examples, following which we propose the inversion-based method for analyzing the identifiability (i.e., invertibility) of the time-varying parameters and analyze its computing complexity. Section IV provides two examples, a one-qubit system with single input and a two-qubit system with multiple inputs, to show the advantage of the inversion-based method—how the singularity problem can be solved by abundant measurements and analyzing the influence of noise. Finally, conclusions are drawn in Sec. V.

II. A DIRECT IDENTIFICATION SCHEME VIA RAMSEY INTERFEROMETRY

Let us start from a simple case. Suppose that the time-varying parameter $u(t)$ to be identified is coupled to a single-qubit probe [29], and we expect to read out $u(t)$ through the time-resolved measurement of the qubit. A simple model for the readout process can be described by the Schrödinger equation $\dot{\psi}(t) = -iH(t)\psi(t)$, where $\psi(t)$ is the quantum state of the qubit probe and

$$H(t) = u(t)\sigma_z. \tag{1}$$

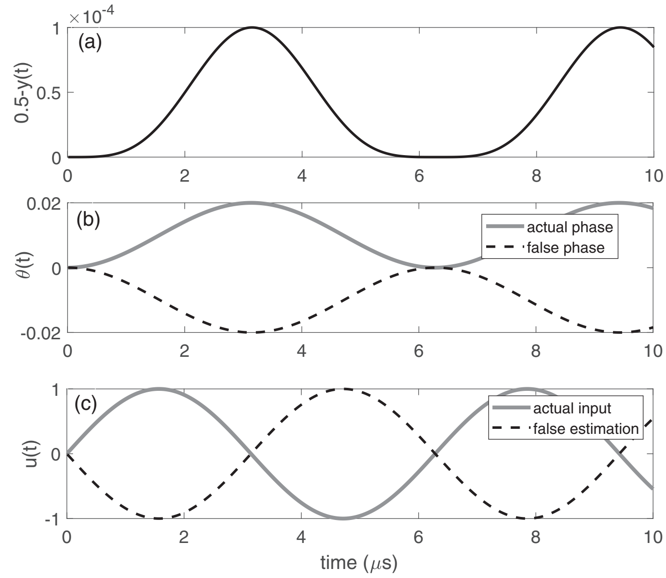

FIG. 2. Ramsey-experiment-based identification. The measured output (a) corresponds to two different time traces of the qubit phase (b) in which one is false. The resulting identified *in situ* input (c) is thus undecidable.

Here, $\sigma_x, \sigma_y, \sigma_z$ are the standard Pauli matrices. The qubit is prepared at the superposition state $\psi(0) = \frac{1}{\sqrt{2}}(|0\rangle + |1\rangle)$ and evolves as follows:

$$\psi(t) = \frac{1}{\sqrt{2}}[e^{-i\theta(t)/2}|0\rangle + e^{i\theta(t)/2}|1\rangle], \tag{2}$$

where the information about $u(t)$ is transferred to the accumulated phase

$$\theta(t) = \int_0^t u(\tau)d\tau. \tag{3}$$

In the laboratory, the phase $\theta(t)$ can be conveniently measured via a Ramsey experiment that corresponds to the expectation value of σ_x:

$$y(t) = \langle\psi(t)|\sigma_x|\psi(t)\rangle = \frac{\cos\theta(t)}{2}. \tag{4}$$

Reversing the above processes, we obtain the identification formula:

$$u(t) = \frac{d}{dt}[\pm\arccos 2y(t) + k\pi] = \frac{\mp\dot{y}(t)}{\sqrt{1-4y^2(t)}}. \tag{5}$$

There are two issues in this identification scheme. First, the identification formula (5) provides two solutions among which one cannot determine which one is correct, because the involved cosine function in Eq. (4) is not one-to-one. For example, as is shown in Fig. 2, the two different signals $u(t) = \pm\sin\omega_0 t$ $(\omega_0 = 1)$ accumulate different traces of phases that lead to the same measured output $y(t)$, and we are not able to judge whether $u(t) = \sin\omega_0 t$ or $u(t) = -\sin\omega_0 t$ is the real *in situ* signal. In practice, the false solution may be easily excluded via prior knowledge, but later we will see that the signal is actually identifiable.

Second, this direct identification scheme relies on the analytical solvability of the time-dependent Schrödinger Eq. (1), which is usually impossible when $H(t)$ and $H(t')$ do not commute for $t \neq t'$. For example, the *in situ* signal cannot be simply encoded into the qubit phase when there is a bias term in the qubit probe Hamiltonian:

$$H(t) = \omega_0\sigma_x + u(t)\sigma_z. \tag{6}$$

This issue is even more severe in multiqubit systems that are coupled with multiple input signals. Therefore a more general framework is required to analyze the invertibility.

III. INVERSION-BASED IDENTIFICATION OF TIME-VARYING SIGNALS

In this section we will formulate the identification problem as an inverse problem of solving the output of the dynamical Schrödinger equation. The invertibility criterion will be derived as well as the inversion algorithm for extracting the signals.

A. The invertibility of quantum systems

To facilitate the following derivation, we assume that the probe system is a closed or a Markovian open system, so that the evolution can be described by

$$\dot\rho(t) = [\mathcal{L}_0 + u(t)\mathcal{L}_1]\rho(t), \tag{7}$$

where the density matrix is initially prepared at $\rho(0) = \rho_0$. The superoperators $\mathcal{L}_0$ and $\mathcal{L}_1$, which are assumed to be precisely known, are a Liouvillian ($\mathcal{L}\rho = -i[H,\rho]$ with H being the interaction Hamiltonian) or a Lindbladian (i.e., $\mathcal{L}\rho = 2L\rho L^\dagger - L^\dagger L\rho - \rho L^\dagger L$ with L being the coupling operator). We expect to identify $u(t)$ from the time-resolved ensemble measurement

$$y(t) = \langle O\rangle \triangleq \mathrm{Tr}[\rho(t)O], \tag{8}$$

where O is the corresponding observable.

The system is said to be left invertible (or functional observable) if for any admissible $u(t) \neq u'(t)$, their resulting outputs $y(t) \neq y'(t)$. To determine whether the system is invertible, we can differentiate the measurement signal $y(t)$, which yields

$$\dot y(t) = \langle \mathcal{L}_0^* O\rangle + \langle \mathcal{L}_1^* O\rangle u(t), \tag{9}$$

where $\mathcal{L}_k^* O$ $(k = 0, 1)$ represents the adjoint operation of $\mathcal{L}_k$ on the observable O, i.e., $\mathrm{Tr}[(\mathcal{L}\rho)O] = \mathrm{Tr}[\rho(\mathcal{L}^*O)] = \langle\mathcal{L}^*O\rangle$. For example, when $\mathcal{L}$ is a Liouvillian operator, i.e., $\mathcal{L}\rho = -i[H,\rho]$, we can derive $\mathcal{L}^*O = i[H,O]$ from

$$\mathrm{Tr}\{(\mathcal{L}\rho)O\} = \mathrm{Tr}\{-i[H,\rho]O\} = \mathrm{Tr}\{[H,O]\rho\}. \tag{10}$$

Similarly, the adjoint operation of a Lindbladian $\mathcal{L}\rho = 2L\rho L^\dagger - \rho L^\dagger L - L^\dagger L\rho$ on some observable O is $\mathcal{L}^*O = 2L^\dagger OL - OL^\dagger L - L^\dagger LO$.

If it happens that $\langle\mathcal{L}_1^*O\rangle \equiv 0$, we can go on to differentiate $\dot y(t) = \langle\mathcal{L}^*O\rangle$ α times until $\langle\mathcal{L}_1^*(\mathcal{L}_0^*)^{\alpha-1}O\rangle \neq 0$, which gives

$$y^{(\alpha)}(t) = \langle(\mathcal{L}_0^*)^\alpha O\rangle + \langle\mathcal{L}_1^*(\mathcal{L}_0^*)^{\alpha-1}O\rangle u(t). \tag{11}$$

The index α is called the relative degree of the quantum system. It can be proved that the system is left invertible if and only if its relative degree is finite (in fact, α is always no greater than the system's dimension n if it is finite) [34], which is exactly the condition of identifiability for uniquely estimating time-varying input signals.

In practice, it is inconvenient to calculate the values of $\langle\mathcal{L}_1^*(\mathcal{L}_0^*)^kO\rangle$ $(k \geqslant 0)$ because $\rho(t)$ is usually not analytically solvable. Since the invertibility condition holds for any $u(t)$ and $\rho(0)$, we can equivalently verify it by the operators $\mathcal{L}_1^*(\mathcal{L}_0^*)^kO$ instead of their expectation values, i.e., the system is invertible if and only if there exists some finite integer such that $\mathcal{L}_0^*(\mathcal{L}_1^*)^\alpha O \neq 0$ but $\mathcal{L}_0^*(\mathcal{L}_1^*)^kO = 0$ for $k = 0,\ldots,\alpha-1$.

It is natural to extend the invertibility criterion to general systems that involve multiple input and output signals, where the invertibility is also determined by the finiteness of the system's relative degree, although the calculation of the relative degree is much more complicated (see Appendix for details). In addition, we can draw a useful necessary condition from the derivation that the number of time-varying outputs must be no less than that of time-varying input signals. This is to say, one can never uniquely identify m unknown input signals with time-resolved measurements on less than m observables. As will be seen later, in practice we often need to select more than m observable so as to avoid ill-conditioned numerical issues.

B. The inversion-based identification algorithm

The above invertibility analysis also provides an inversion algorithm that can be used to identify the input signal $u(t)$. To see how this can be done, we can solve $u(t)$ from Eq. (11) as

$$u(t) = \phi[\rho(t), y^{(\alpha)}(t)] = \frac{y^{(\alpha)}(t) - \langle(\mathcal{L}_0^*)^\alpha O\rangle}{\langle\mathcal{L}_1^*(\mathcal{L}_0^*)^{\alpha-1}O\rangle}, \tag{12}$$

in which $y^{(\alpha)}(t)$ can be directly calculated from the measurement output $y(t)$, and the terms $\langle(\mathcal{L}_0^*)^\alpha O\rangle$ and $\langle\mathcal{L}_1^*(\mathcal{L}_0^*)^{\alpha-1}O\rangle$ are also physically measurable quantities. Therefore one can perform the corresponding time-resolved measurements on observables $(\mathcal{L}_0^*)^\alpha O$ and $\mathcal{L}_1^*(\mathcal{L}_0^*)^{\alpha-1}O$ and use Eq. (12) to reconstruct $u(t)$.

Under the circumstance that the observables $(\mathcal{L}_0^*)^\alpha O$ and $\mathcal{L}_1^*(\mathcal{L}_0^*)^{\alpha-1}O$ are difficult to measure, one can also replace Eq. (12) back into Eq. (7), leading to the so-called inverse system:

$$\dot\rho(t) = \{\mathcal{L}_0 + \phi[\rho(t), y^{(\alpha)}(t)]\mathcal{L}_1\}\rho(t), \tag{13}$$

in which $y(t)$ acts as the input and $u(t)$ acts as the output. We can first numerically solve it from the measurement data of $y(t)$ and the prepared initial state $\rho(0)$ and use the calculated $\rho(t)$ to reconstruct $u(t)$ via Eq. (12).

For illustration, we apply the inverse-system analysis to the example discussed in Sec. II. The differential of $y(t) = \langle\psi(t)|\sigma_x|\psi(t)\rangle$ yields

$$u(t) = -\frac{\dot y(t)}{\langle\psi(t)|\sigma_y|\psi(t)\rangle}, \tag{14}$$

which indicates that the system's relative degree is 1, and hence the system is invertible at least on a nonempty time interval, as long as $\langle\psi(t)|\sigma_y|\psi(t)\rangle$ is initially nonzero. Hence the signal is in principle identifiable via the inversion algorithm, but the Ramsey-experiment-based scheme may fail.

To better understand the identification, we show that the system may lose invertibility under improper measurements, e.g., when $y(t) = \langle\psi(t)|\sigma_z|\psi(t)\rangle$. One can verify that the relative degree $\alpha = \infty$ and thus $u(t)$ can never be uniquely identified from this measurement. However, when a bias Hamiltonian is introduced, i.e.,

$$\dot{\psi}(t) = -i[\omega_b\sigma_x + u(t)\sigma_z]\psi(t), \tag{15}$$

the system can regain invertibility under the same measurement. In such a case we can differentiate $y(t)$ twice to obtain

$$u(t) = \frac{\omega_b\langle\psi(t)|\sigma_z|\psi(t)\rangle - \omega_0^{-1}\ddot{y}(t)}{\langle\psi(t)|\sigma_x|\psi(t)\rangle}, \tag{16}$$

which indicates that the system's relative degree is $\alpha = 2$ and hence the signal $u(t)$ is identifiable.

This example shows that the signal is in principle identifiable by introducing the bias Hamiltonian. In practice, we always prefer the lowest-relative-degree identification schemes [e.g., using (14)] instead of Eq. (16), if experimentally allowed, to reduce high-frequency noise induced errors from the numerical differentiation of time-varying signals.

Let us compare the inversion method with the commonly used nonlinear regression method that estimates $u(t)$ by minimizing the following regression functional:

$$\mathcal{D}[u(t)] = \int_0^T \|y_{\rm exp}(t) - F[u(t)]\|^2 dt, \tag{17}$$

where $y_{\rm exp}(t)$ is the experimentally measured output, and $F[u(t)]$ represents the output calculated from system (7) using $u(t)$. The regression index can be iteratively minimized by standard gradient-descent algorithms starting from an initial guess on $u(t)$. In comparison, the proposed inversion method has the following twofold advantages in the computational complexity.

First, the inversion method is performed in a "single-shot" manner in that the differential Eq. (13) is to be numerically solved only for once, while the nonlinear regression method has to solve Eq. (7) in every iteration. Although the differential equation to be integrated is more complicated, the numerical computational burden is slightly increased by the calculation of $\phi[\rho(t), y^{(\alpha)}(t)]$, whose algebraic form is known and the numerical differentiation of $y(t)$ [to obtain $y^{(\alpha)}(t)$]. Comparing the potentially large number of iterations in the regression approach, the "single-shot" integration in the inversion method is much cheaper.

Second, the nonlinear regression method is highly dependent on the initial guess on $u(t)$, which may lead to a false estimation due to potential local traps. The inversion method, which is performed in a "single-shot" manner, does not have this problem. It should be noted that the inversion algorithm can become instable due to the singularity of Eq. (12), e.g., when the denominator crosses zero in Eq. (14). This is an intrinsic property of the system that can be relieved by introducing extra measurements (e.g., using two outputs to identify one input), but it cannot be overcome by any algorithm.

Since practical measurement of $y(t)$ is always sampled in discrete time, the sampling rate must be sufficiently high (according Shannon's sampling Theorem [42]) so as to faithfully recover the signal, following which a low-pass filter is required to mitigate the influence of high-frequency noises on the numerical differentiation. As for the numerical differentiation schemes, we can use the simplest two-point difference,

$$\dot{y}(t_k) \approx \frac{y(t_{k+1}) - y(t_k)}{\Delta t}, \tag{18}$$

between adjacent sampling points, where $t_k = k\Delta t$ with Δt being the sampling period. To improve the precision, one can use the more advanced three-point formula [43]

$$\dot{y}(t_k) \approx \begin{cases} \frac{-3y(t_1)+4y(t_2)-y(t_3)}{2\Delta t}, & k = 1 \\ \frac{-y(t_{k-1})+y(t_{k+1})}{2\Delta t}, & 1 < k < N \\ \frac{y(t_{N-2})-4y(t_{N-1})+3y(t_N)}{2\Delta t}, & k = N, \end{cases} \tag{19}$$

where N is the number of time steps. As will be seen in the following simulations, the adoption of three-point differentiation also improves the stability of the inversion algorithm.

IV. NUMERICAL EXAMPLES

In this section we show how the proposed inversion algorithm can be applied to identify single or multiple time-varying signals in two-qubit quantum systems. Suppose that the system to be probed consists of two coupled transmon qubits with the following Hamiltonian [44]:

$$H = \frac{\omega_1(t)}{2}\sigma_{1z} + \frac{\omega_2(t)}{2}\sigma_{2z} + g(t)(\sigma_{1+}\sigma_{2-} + \sigma_{1-}\sigma_{2+}), \tag{20}$$

where σ_z and $\sigma_\pm$ are the standard Pauli and lowering or raising operators. The signals $\omega_1(t)$, $\omega_2(t)$, and $g(t)$ to be identified are the frequencies of the two qubits and the effective qubit-qubit coupling strength that are tunable by external electronic dc sources. In the following, we will apply the inversion

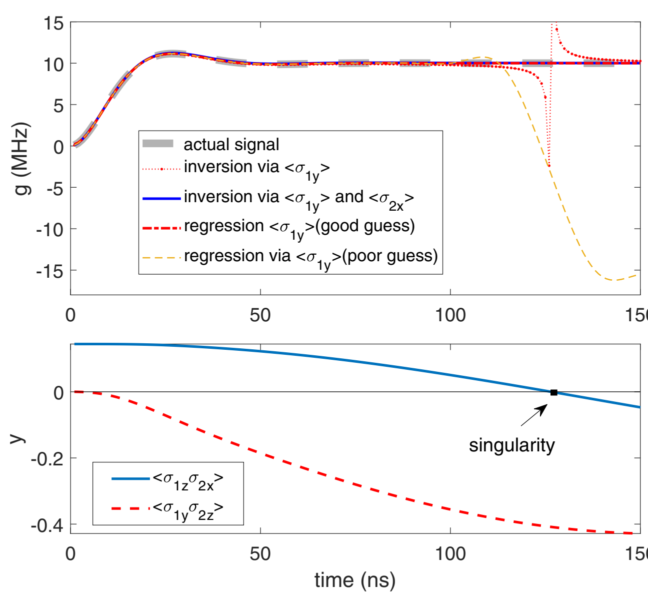

FIG. 3. Identification of the *in situ* signal by using inversion method and regression method and the denominators in the inversion method. The identified signal by using inversion method by using single measurement and regression method with a good and a bad initial guess on $g(t)$, respectively. The identification encounters singularity at around $t = 130$ ns.

algorithm to the identification of single-input and multi-input signals.

A. Identification of single *in situ* signals

In this case we fix $\omega_1(t) = \omega_2(t) \equiv 1$ MHz and identify the time-varying $g(t)$ from time-resolved measurements. As shown in Fig. 3, the signal $g(t)$ to be identified is chosen to be a distorted step function rising from 0 to 10 MHz, which is often applied for quickly switching on the qubit-qubit coupling.

The initial state of the system is chosen to be

$$|\psi(0)\rangle = \left(\sqrt{\frac{2}{3}}|0\rangle + \sqrt{\frac{1}{3}}|1\rangle\right) \otimes \left(\frac{\sqrt{3}}{2}|0\rangle + \frac{1}{2}|1\rangle\right),$$

and the time-resolved measurement of σ_{1y} is performed on the first qubit. One can derive that the corresponding relative order is $\alpha = 1$ and the mapping $\phi[\rho(t), \dot{y}(t)]$ used for inversion is

$$\phi[\rho(t), \dot{y}(t)] = -\frac{1}{2}\frac{\dot{y}(t) + \langle\sigma_{1x}\rangle}{\langle\sigma_{1z}\sigma_{2x}\rangle}, \tag{21}$$

where the notation defined in (8) is applied.

In the numerical simulations, we apply Euler's algorithm to solve the nonlinear differential equation and the two-point method to numerically differentiate $y(t)$. The simulation results are shown in Fig. 3, in which the identified signal $g(t)$ encounters singularity in the matrix inversion in Eq. (A5). At the critical time $t \approx 120$ ns [see Fig. 3(b)], the numerical simulation becomes instable, but it still comes back later to the true solution. The inversion may be more stable by more precisely integrating the nonlinear differential equation, but there is no guarantee for the inversion algorithm to get over the singularity.

We also make comparisons with the nonlinear regression method that starts from a good initial guess $g^{(0)}(t) \equiv 10$ MHz and a poor initial guess $g^{(0)}(t) \equiv -10$ MHz, respectively. It is found that the former converges to the true signal, but the latter diverges away just around the critical time.

Therefore both the inversion and the regression methods can well identify the *in situ* signal before the critical time and may fail after it. The inversion algorithm is more efficient because it integrates the differential equation for only once without having to guess the signal in the beginning, but the regression method needs to solve the differential equation repeatedly until convergence.

To avoid the singularity, we may introduce redundant measurements to collect more information about the input signal. In the simulation, we use two measurements $y_1(t) = \langle\sigma_{1y}\rangle$, $y_1(t) = \langle\sigma_{2x}\rangle$, under which the mapping $\phi[\rho(t), \dot{\vec{y}}(t)]$ for inversion is

$$\phi[\rho(t), \dot{\vec{y}}(t)] = \frac{1}{2}\cdot\frac{\langle\sigma_{1y}\sigma_{2z}\rangle(\dot{y}_2(t) - \langle\sigma_{2y}\rangle) - \langle\sigma_{1z}\sigma_{2x}\rangle(\dot{y}_1(t) + \langle\sigma_{1x}\rangle)}{\langle\sigma_{1z}\sigma_{2x}\rangle^2 + \langle\sigma_{1y}\sigma_{2z}\rangle^2}. \tag{22}$$

It can be seen that the denominator crosses zero only when $\langle\sigma_{1z}\sigma_{2x}\rangle$ and $\langle\sigma_{1y}\sigma_{2z}\rangle$ simultaneously vanish, which is highly unlikely in general cases. As is seen in Fig. 3, the inversion algorithm can precisely reproduce the *in situ* signal from redundant measurements, in which either $\langle\sigma_{1z}\sigma_{2x}\rangle$ or $\langle\sigma_{1y}\sigma_{2z}\rangle$ may cross zero, but they do not vanish at the same time.

B. Simultaneous identification of multiple *in situ* signals

Assume that the *in situ* time-varying signals $\omega_1(t)$, $\omega_2(t)$, and $g(t)$ are all unknown. To identify them simultaneously, we need at least three time-resolved measurements and, according to the analysis in Appendix, the system is invertible with relative degree $\alpha = 1$ when $\vec{\mathcal{L}}_c^* O_1$, $\vec{\mathcal{L}}_c^* O_2$, and $\vec{\mathcal{L}}_c^* O_3$ are linearly independent with each other, where $\vec{O} = (O_1, O_2, O_3)$ are the chosen observables. A viable choice is as follows:

$$\vec{O} = (\sigma_{1x}, \sigma_{1y}, \sigma_{2x})^T, \tag{23}$$

under which the mapping $\phi[\rho(t), \dot{\vec{y}}(t)]$ for inversion is

$$\phi[\rho(t), \dot{\vec{y}}(t)] = \begin{pmatrix} \langle\sigma_{1y}\rangle & 0 & -2\langle\sigma_{1z}\sigma_{2y}\rangle \\ -\langle\sigma_{1x}\rangle & 0 & 2\langle\sigma_{1z}\sigma_{2x}\rangle \\ 0 & \langle\sigma_{2y}\rangle & -2\langle\sigma_{1y}\sigma_{2z}\rangle \end{pmatrix}^{-1} \begin{pmatrix} \dot{y}_1(t) \\ \dot{y}_2(t) \\ \dot{y}_3(t) \end{pmatrix}. \tag{24}$$

We simulate the identification process for *in situ* signals $\omega_1(t)$, $\omega_2(t)$, and $g(t)$, which are all chosen as distorted step functions. As is shown in Fig. 4, the identified signals all conform to the true ones until the first critical time $t \approx 70$ ns when singularity occurs. They come back to the true signals after a spiky deviation and again encounter singularity at the second critical time $t \approx 200$ ns. The inaccuracy caused by the singularities can be reduced by introducing two time-resolved measurements $O_4 = \sigma_{2y}$ and $O_5 = \sigma_{1z}$ or by using the three-point differential of $y(t)$.

C. The affection of noises

The prevalently existing noises in realistic quantum systems can affect the quality of identification or even destroy it. Taking the one-qubit probe as an example, we consider two typical classes of noises present in the following system:

$$\dot{\psi}(t) = -i[\mathbf{n}_e(t)\sigma_z + u(t)\sigma_z]\psi(t), \tag{25}$$

$$y(t) = \langle\psi(t)|\sigma_x|\psi(t)\rangle + \mathbf{n}_m(t). \tag{26}$$

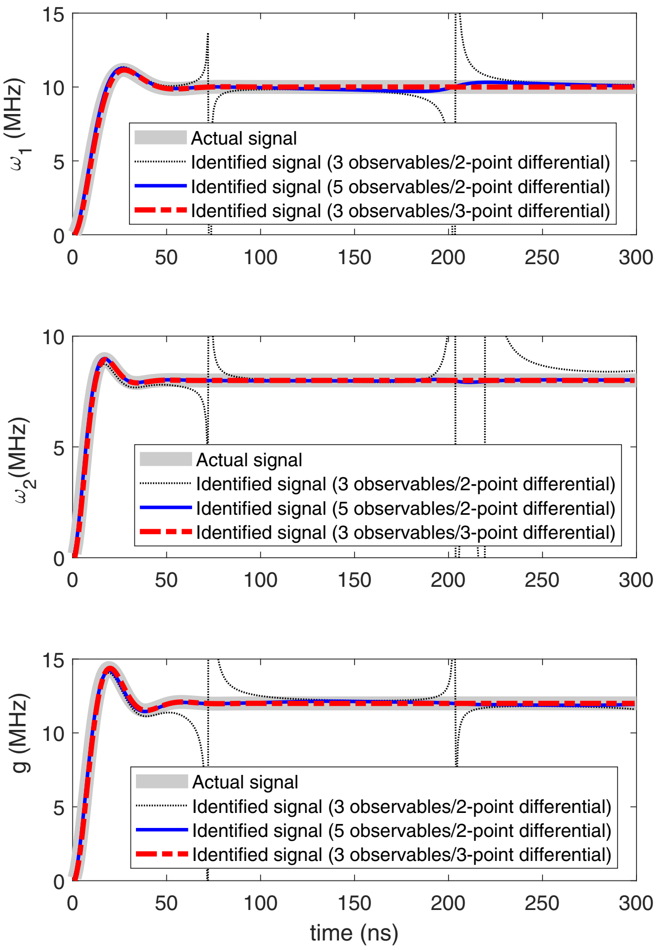

FIG. 4. The identification of multiple *in situ* signals $\omega_1(t)$, $\omega_2(t)$, and $g(t)$ (all chosen as distorted step functions) in a two-qubit system via measurements on three and five observables. Singularities appear in the three-observable case when a two-point differential is used (red dashed line), but they disappear in the five-observable case (blue solid line) or three-observable case using three-point differentials (yellow dashed line).

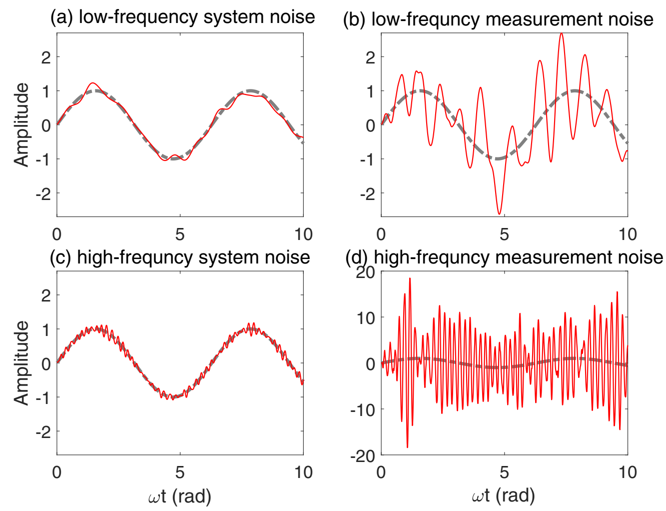

FIG. 5. (a) The calculated *in situ* signal when there is low-frequency system noise ($\mathbf{n}_e$). (b) The calculated *in situ* signal when there is high-frequency system noise. (c) The calculated *in situ* signal when there is low-frequency measurement noise ($\mathbf{n}_m$). (d) The calculated *in situ* signal when there is high-frequency measurement noise.

The noise $\mathbf{n}_e(t)$ comes from unwanted coupling to unspecified signals (e.g., crosstalk via some other qubit's input), and $\mathbf{n}_m(t)$ comes from the measurement noise. According to Eq. (12), the measurement noise, especially its high-frequency components, can have a fatal effect on the quality of readout results because it can be greatly amplified by the differential of $y(t)$. The system is less affected by the high-frequency components of noise $\mathbf{n}_e(t)$ because they tend to be filtered.

In the simulation we simulated low-frequency (comparable with the frequency of the signals) and high-frequency (25–30 times the frequency of the signals) random noise in system ($\mathbf{n}_e(t)$). The variance of the noise is taken to be 10^{-2} for $n_e(t)$ and 10^{-6} for $n_m(t)$, respectively. As shown in Fig. 5, the measurement noise distorts the calculated *in situ* signal dramatically even with a smaller variance, especially when the frequency is high. To improve the accuracy, the measurement noises must be effectively filtered. By contrast, the high-frequency noises in the system have a minor affect on the identification. Therefore, in practice, the measured output should be carefully filtered to reduce the noise affect while keeping the signal undistorted as much as possible.

V. CONCLUSION

To conclude, we propose an inverse-system-based method to unambiguously identify time-varying parameters from time-resolved measurements which is experiment friendly. Although the parameters are usually locally identifiable (i.e., likely diverge at some critical time due to the singularity), the proposed method still greatly generalizes the existing Ramsey-experiment-based schemes to arbitrary multi-input–multi-output systems, as long as the algebraic invertibility condition is satisfied. The simulation results show that it can perfectly extract the *in situ* signal in both single-input and multiple-input systems by integrating the nonlinear Schrödinger equation. Although, the algorithm is applicable only on a finite time interval due to potential singularity, one can properly introduce redundant measurements to prolong the applicable time interval. The affection and limitation brought by system's noises are also analyzed through numerical simulations.

The method we developed can be naturally generalized to any other quantum systems, no matter closed or open, as long as the probe system can be precisely modeled and the modeled system is invertible. In principle, one can freely choose the time-resolved measurements for identifying the time-varying parameters according to the invertibility condition. However, in practice one should pick those with lowest relative degree so as to minimize the influence of measurement noise.

ACKNOWLEDGMENT

The authors acknowledge support from National Key Research and Development Program of China (Grant No.

2018YFA0306703), NSFC (Grants No. 61833010 and No. 61773232), and a grant from the Institute for Guo Qiang, Tsinghua University.

APPENDIX: MULTI-INPUT MULTI-OUTPUT INVERSION

Suppose that the quantum system has multiple parameters that are to be identified from multiple time-resolved measurements, as follows that

$$\dot{\rho}(t) = [\mathcal{L}_0 + \vec{u}(t)\cdot\vec{\mathcal{L}}_c]\rho(t), \tag{A1}$$

in which *in situ* signals $\vec{u}(t) = [u_1(t), \dots, u_m(t)]^T$ are coupled to the system via Liouvillians (or Lindbladians) $\vec{\mathcal{L}}_c = (\mathcal{L}_1, \dots, \mathcal{L}_m)$. The dot product is referred to as the inner product $\vec{u}(t)\cdot\vec{\mathcal{L}}_c = \sum_{k=1}^m u_k(t)\mathcal{L}_k$. We expect to identify these signals from n measurements $\vec{y}(t) = [y_1(t), \dots, y_n(t)]^T$, with $y_\ell(t) = \langle O_\ell\rangle$ being the expectation value of the corresponding observable O_ℓ.

Similarly, the quantum system is said to be invertible if for any two different input vectors $\vec{u}(t) \neq \vec{u}'(t)$, the resulting output vectors $\vec{y}(t) \neq \vec{y}'(t)$. According to Eq. (A1), we differentiate $\vec{y}(t)$ and obtain

$$\dot{\vec{y}} = \langle\mathcal{L}_0^*\vec{O}\rangle + \langle\vec{\mathcal{L}}_c^*\vec{O}\rangle\vec{u}, \tag{A2}$$

where

$$\langle\vec{\mathcal{L}}_c^*\vec{O}\rangle = \begin{pmatrix}\langle\vec{\mathcal{L}}_c^*O_1\rangle\\ \vdots \\ \langle\vec{\mathcal{L}}_c^*O_n\rangle\end{pmatrix}, \tag{A3}$$

with

$$\langle\vec{\mathcal{L}}_c^*O_k\rangle = (\langle\mathcal{L}_1^*O_k\rangle, \cdots, \langle\mathcal{L}_m^*O_k\rangle) \tag{A4}$$

for $k = 0, 1, 2, \dots, m$. Similarly, since it is hard to evaluate the expectations, we analyze the corresponding operators. We say that operator arrays $\vec{\mathcal{L}}_c^*O_{i_1}, \dots, \vec{\mathcal{L}}_c^*O_{i_p}$ are linearly independent if

$$\lambda_1\vec{\mathcal{L}}_c^*O_{i_1} + \cdots + \lambda_p\vec{\mathcal{L}}_c^*O_{i_p} \neq 0$$

for any nonzero real numbers $\lambda_1, \dots, \lambda_p$, and the rank of a group of operator arrays is referred to as the maximal number of mutually independent arrays in them. If there exist m mutually linear independent arrays among $\vec{\mathcal{L}}_c^*O_1, \dots, \vec{\mathcal{L}}_c^*O_n$, i.e., $rank(\vec{\mathcal{L}}_c^*\vec{O}) = m$, then the signals can be formally calculated as a regression solution of (A2):

$$\begin{aligned}\vec{u}(t) &= \vec{\phi}[\rho, \dot{\vec{y}}]\\ &= [\langle\vec{\mathcal{L}}_c^*\vec{O}\rangle^T\langle\vec{\mathcal{L}}_c^*\vec{O}\rangle]^{-1}\langle\vec{\mathcal{L}}_c^*\vec{O}\rangle[\dot{\vec{y}} - \langle\mathcal{L}_0^*\vec{O}\rangle].\end{aligned} \tag{A5}$$

This formula is then replaced back to Eq. (A1) to obtain the following inverse system:

$$\dot{\rho}(t) = \{\mathcal{L}_0 + \vec{\phi}[\rho(t), \dot{\vec{y}}(t)]\cdot\vec{\mathcal{L}}_c\}\rho(t). \tag{A6}$$

Similar to the single-input–single-output systems, the expectation $\langle\vec{\mathcal{L}}_c^*\vec{O}\rangle$ may become rank deficient at some time instance even when the operator rank condition $rank(\vec{\mathcal{L}}_c^*\vec{O}) = m$ is satisfied. The affection of singularity on the identification process will be discussed in the following simulation section. Moreover, the operator rank of $\vec{\mathcal{L}}_c^*\vec{O}$ may also be lower than m, under which circumstance Eq. (A5) has no unique solutions for all time t. In such a case, we need to extract $\vec{u}(t)$ via higher-order derivatives of $\vec{y}(t)$. To do this, we first divide $\vec{O} = (\vec{O}_1, \tilde{O}_1)$ such that

$$rank[\vec{\mathcal{L}}_c^*\vec{O}_1] = rank[\vec{\mathcal{L}}_c^*\vec{O}],$$

and $\vec{\mathcal{L}}_c^*\tilde{O}_1$ is linearly dependent with the arrays of $\vec{\mathcal{L}}_c^*\vec{O}_1$, i.e., there exists a matrix V_{11} such that $\vec{\mathcal{L}}_c^*\tilde{O}_1 = V_{11}\vec{\mathcal{L}}_c^*\vec{O}_1$.

Let $\vec{y}_1 = \langle\vec{O}_1\rangle$ and $\tilde{y}_1 = \langle\tilde{O}_1\rangle$. We differentiate them

$$\langle\mathcal{L}_0^*\vec{O}_1\rangle + \langle\vec{\mathcal{L}}_c^*\vec{O}_1\rangle\vec{u} = \dot{\vec{y}}_1 \tag{A7}$$

$$\langle\mathcal{L}_0^*\tilde{O}_1\rangle + \langle\vec{\mathcal{L}}_c^*\tilde{O}_1\rangle\vec{u} = \dot{\tilde{y}}_1, \tag{A8}$$

and then eliminate $\vec{u}$ in the second equation using the relation $\vec{\mathcal{L}}_c^*\tilde{O}_1 = V_{11}\vec{\mathcal{L}}_c^*\vec{O}_1$, which gives $\bar{y}_2 = \langle\bar{O}_2\rangle$, where

$$\bar{O}_2 = \mathcal{L}_0^*\tilde{O}_1 - V_{11}\mathcal{L}_0^*\vec{O}_1, \quad \bar{y}_2 = \dot{\tilde{y}}_1 - V_{11}\dot{\vec{y}}_1.$$

This equation can be further differentiated to produce a new group of linear equations of $\vec{u}$:

$$\langle\mathcal{L}_0^*\bar{O}_2\rangle + \langle\vec{\mathcal{L}}_c^*\bar{O}_2\rangle\vec{u} = \dot{\bar{y}}_2. \tag{A9}$$

If $\vec{\mathcal{L}}_c^*\vec{O}_1$ and $\vec{\mathcal{L}}_c^*\bar{O}_2$ include m linearly independent rows of operators, we can let $\vec{O}_2 = \bar{O}_2$ and halt the process. Otherwise, we can do the same operation on $\bar{O}_2$ by separating its linearly independent part. Inductively, if the system is invertible, we can obtain a transformation $\vec{O}' = V\vec{O} = (\vec{O}_1, \dots, \vec{O}_\alpha)^T$ of the observables after repeatedly doing the above differentiation process, which leads to the following group of equations:

$$\begin{gathered}\langle\mathcal{L}_0^*\vec{O}_1\rangle + \langle\vec{\mathcal{L}}_c^*\vec{O}_1\rangle\vec{u} = f_1[\vec{y}^{(1)}, \dots, \vec{y}^{(\alpha_r)}]\\ \vdots\\ \langle\mathcal{L}_0^*\vec{O}_\alpha\rangle + \langle\vec{\mathcal{L}}_c^*\vec{O}_\alpha\rangle\vec{u} = f_n[\vec{y}^{(1)}, \dots, \vec{y}^{(\alpha_r)}],\end{gathered}$$

in which

$$rank(\vec{\mathcal{L}}_c^*\vec{O}') = m \tag{A10}$$

and $\vec{y}_k = f[\vec{y}^{(1)}, \dots, \vec{y}^{(\alpha_k)}]$, $k = 1, \dots, r$, are linear functions of the derivatives of $\vec{y}$ with $\alpha_1 < \cdots < \alpha_r$. The required highest order of differentiation, α_r, is defined as the relative degree of the multi-input–multi-output system. The system is invertible if and only if the relative degree is finite.

The above inversion process also reveals that to guarantee the transformation of observables exists, the number of measurement outputs must not be less than m. In practice, one can introduce redundant time-resolved measurements (i.e., $n > m$), which may reduce the risk of encountering singularity. This will be shown in the numerical simulations.

[1] K. Banaszek, M. Cramer, and D. Gross, New J. Phys. **15**, 125020 (2013).

[2] A. Anis and A. I. Lvovsky, New J. Phys. **14**, 105021 (2012).

[3] A. M. Brańczyk, D. H. Mahler, L. A. Rozema, A. Darabi, A. M. Steinberg, and D. F. V. James, New J. Phys. **14**, 085003 (2012).

[4] K. Maruyama, D. Burgarth, A. Ishizaki, T. Takui, and K. B. Whaley, Quantum Inf. Comput. **12**, 763 (2012).

[5] Y. Wang, B. Qi, D. Dong, and I. R. Petersen, in *Proceedings of the 2016 IEEE 55th Conference on Decision and Control (CDC)* (IEEE, Piscataway, NJ, 2016), pp. 2523–2528.

[6] S.-Y. Hou, H. Li, and G.-L. Long, Sci. Bull. **62**, 863 (2017).

[7] C. Le Bris, M. Mirrahimi, H. Rabitz, and G. Turinici, ESAIM. Control. Optim. Calc. Var. **13**, 378 (2007).

[8] J. Zhang and M. Sarovar, Phys. Rev. Lett. **113**, 080401 (2014).

[9] O. F. Alis, H. Rabitz, M. Q. Phan, C. Rosenthal, and M. Pence, J. Math. Chem. **35**, 65 (2004).

[10] R. B. Wu, T. F. Li, A. G. Kofman, J. Zhang, Y.-X. Liu, Y. A. Pashkin, J.-S. Tsai, and F. Nori, Phys. Rev. A **87**, 022324 (2013).

[11] R. L. Kosut, I. A. Walmsley, and H. Rabitz, IFAC Proc. **38**, 668 (2005).

[12] Y. Wang, D. Dong, and H. Yonezawa, in *Proceedings of the 2019 IEEE 58th Conference on Decision and Control (CDC)* (IEEE, Piscataway, NJ, 2019), pp. 396–400.

[13] J. Martinis, Y. Chen, H. Neven, and D. Kafri, Nonlinear Calibration of a Quantum Computing Apparatus, Patent No. AU 2017/420803 A1.

[14] R. Kosut, H. Rabitz, and I. Walmsley, IFAC Proc. **36**, 121 (2003).

[15] B. R. Johnson, *Controlling Photons in Superconducting Electrical Circuits* (Yale University, New Haven, CT, 2011).

[16] I. N. Hincks, C. E. Granade, T. W. Borneman, and D. G. Cory, Phys. Rev. Appl. **4**, 024012 (2015).

[17] F. Motzoi, J. M. Gambetta, S. T. Merkel, and F. K. Wilhelm, Phys. Rev. A **84**, 022307 (2011).

[18] P. E. Spindler, Y. Zhang, B. Endeward, N. Gershernzon, T. E. Skinner, S. J. Glaser, and T. F. Prisner, J. Magn. Reson. **218**, 49 (2012).

[19] S. Glaser, U. Boscain, T. Calarco, C. P. Koch, W. Köckenberger, R. Kosloff, I. Kuprov, B. Luy, S. Schirmer, T. Schulte-Herbrueggen *et al.*, Eur. Phys. J. D **69**, 279 (2015).

[20] W. Rose, H. Haas, A. Q. Chen, N. Jeon, L. J. Lauhon, D. G. Cory, and R. Budakian, Phys. Rev. X **8**, 011030 (2018).

[21] R. Patterson, A. Hammoud, and M. Elbuluk, Cryogenics **46**, 231 (2006).

[22] R. Patterson, A. Hammoud, J. Dickman, S. Gerber, M. Elbuluk, and E. Overton, Report No. NASA/TM-2003-212600 E-14159 NAS1.15:212600 (2004).

[23] M. Sarovar, T. Proctor, K. Rudinger, K. Young, E. Nielsen, and R. Blume-Kohout, Quantum **4**, 321 (2020).

[24] W. Kong, A kind of superconductive quantum bit regulation method based on crosstalk analysis, Patent No. CN201910704474.7A.

[25] X. Cao, B. Chu, Y.-x. Liu, Z. Peng, and R.-B. Wu, IEEE Transactions on Control Systems Technology, doi: 10.1109/TCST.2021.3060321.

[26] M. A. Rol, L. Ciorciaro, F. Malinowski, B. Tarasinski, R. Sagastizabal, C. C. Bultink, Y. Salath'e, N. Haandbaek, J. Sedivy, and L. DiCarlo, Appl. Phys. Lett. **116**, 054001 (2020).

[27] M. Hofheinz, E. M. Weig, M. Ansmann, R. C. Bialczak, E. Lucero, M. Neeley, A. D. O'Connell, H. Wang, J. M. Martinis, and A. N. Cleland, Nature (London) **454**, 310 (2008).

[28] J. M. Gambetta, A. D. Córcoles, S. T. Merkel, B. R. Johnson, J. A. Smolin, J. M. Chow, C. A. Ryan, C. Rigetti, S. Poletto, T. A. Ohki *et al.*, Phys. Rev. Lett. **109**, 240504 (2012).

[29] D. Vion, A. Aassime, A. Cottet, P. Joyez, H. Pothier, C. Urbina, D. Esteve, and M. Devoret, Fortschr. Phys. **51**, 462 (2003).

[30] R. Hirschorn, IEEE Trans. Autom. Control **24**, 855 (1979).

[31] *Nonlinear Controllability and Optimal Control*, edited by H. Sussmann (Taylor & Francis Group, London, 1990).

[32] L. F. Caudill, H. Rabitz, and A. Askar, Inverse Probl. **10**, 1099 (1994).

[33] R. M. Robinson, D. R. R. Scobee, S. A. Burden, and S. Shankar Sastry, Proc. SPIE, p. 98361 (2016).

[34] C. K. Ong, G. M. Huang, T. J. Tarn, and J. W. Clark, Math. Systems Theory **17**, 335 (1984).

[35] P. Gross, H. Singh, H. Rabitz, K. Mease, and G. M. Huang, Phys. Rev. A **47**, 4593 (1993).

[36] Z. M. Lu and H. Rabitz, J. Phys. Chem. **99**, 13731 (1995).

[37] A. Jha, V. Beltrani, C. Rosenthal, and H. Rabitz, J. Phys. Chem. A **113**, 7667 (2009).

[38] E. Brown and H. Rabitz, J. Math. Chem. **31**, 17 (2002).

[39] W. Zhu, M. Smit, and H. Rabitz, J. Chem. Phys. **110**, 1905 (1999).

[40] W. Zhu and H. Rabitz, J. Chem. Phys. **119**, 3619 (2003).

[41] J. W. Clark, C. K. Ong, T. J. Tarn, and G. M. Huang, Math. Systems Theory **18**, 33 (1985).

[42] A. J. Jerri, Proc. IEEE **65**, 1565 (1977).

[43] R. Burden and J. Faires, *Numerical Analysis* (Cengage Learning, 2011), pp. 174–184.

[44] Y. Wu, L. Yang, M. Gong, Y. Zheng, H. Deng, Z. Yan, Y. Zhao, K. Huang, A. D. Castellano, W. J. Munro *et al.*, npj Quantum Inf. **4**, 50 (2018).